

# Approximability of the Six-vertex Model

Jin-Yi Cai\*

Tianyu Liu<sup>†</sup>

Pinyan Lu<sup>‡</sup>

## Abstract

We take the first step toward a classification of the approximation complexity of the six-vertex model. This is a subject of extensive research in statistical physics. Our result concerns the approximability of the partition function on 4-regular graphs, classified according to the parameters of the model. Our complexity results conform to the phase transition phenomenon from physics. We show that the approximation complexity of the six-vertex model behaves dramatically differently on the two sides separated by the phase transition threshold. Furthermore, we present structural properties of the six-vertex model on planar graphs for parameter settings that have known relations to the Tutte polynomial  $T(G; x, y)$ .

## 1 Introduction

The six-vertex model originates in statistical mechanics for crystal lattices with hydrogen bonds. It is a vertex model family with various parameter settings. Classically it is defined on a planar lattice region where each vertex of the lattice is connected by an edge to four nearest neighbors. A state of the model consists of an arrow on each edge such that the number of arrows pointing inwards at each vertex is exactly two. This 2-in-2-out law on the arrow configurations is called the *ice rule* [33]. Thus there are six permitted types of local configurations around a vertex—hence the name *six-vertex model* (see Figure 1). In graph theoretic terms, the states are Eulerian orientations of the underlying undirected graph.

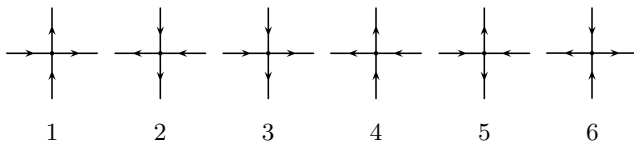


Figure 1: Valid configurations of the six-vertex model.

In general, the six configurations 1 to 6 in Figure 1 are associated with six possible weights  $w_1, \dots, w_6$ . We will follow convention in physics and assume *arrow*

*reversal symmetry*<sup>1</sup>, i.e.  $w_1 = w_2 = a, w_3 = w_4 = b$  and  $w_5 = w_6 = c$ . In this paper we assume  $a, b, c \geq 0$ , as is assumed in classical physics. The partition function of the six-vertex model with parameters  $(a, b, c)$  on a 4-regular graph  $G$ , where incident edges of each vertex are labeled 1 to 4, is defined as

$$Z(G; a, b, c) = \sum_{\tau \in \mathcal{EO}(G)} a^{n_1+n_2} b^{n_3+n_4} c^{n_5+n_6},$$

where  $\mathcal{EO}(G)$  is the set of all Eulerian orientations of  $G$ , and  $n_i$  is the number of vertices in type  $i$  ( $1 \leq i \leq 6$ ) in the graph under an Eulerian orientation  $\tau \in \mathcal{EO}(G)$ .

The first such models were introduced by Linus Pauling [28] in 1935 to describe the properties of ice. In 1967, Elliot Lieb [24, 22, 23] famously showed that, for parameters  $(a, b, c) = (1, 1, 1)$  on the square lattice graph, as the side  $N$  of the square approaches  $\infty$ , the value of the “partition function per vertex”  $W = Z^{1/N^2}$  approaches  $(\frac{4}{3})^{3/2} \approx 1.5396007 \dots$  (this is called Lieb’s square ice constant). This result is called an exact solution of the model, and is considered a triumph. After that, exact solutions for other lattice type graphs (such as [34, 8]) have been obtained in the limiting sense.

For half a century, the six-vertex model has fascinated physicists, chemists, mathematicians and others. Beyond physics, connections of the six-vertex model to many other areas have been discovered. For example, in a celebrated proof, Zeilberger [39] proved the alternating sign matrix (ASM) conjecture in combinatorics. Kuperberg [21] gave a simplified proof making a connection to the six-vertex model.

The six-vertex model is also known to be related to the Tutte polynomial [7] in at least two points. It is known [36] that  $T(G; 0, -2)$  is the number of Eulerian orientations, i.e.,  $T(G; 0, -2) = Z(G; 1, 1, 1) = |\mathcal{EO}(G)|$ , for every 4-regular graph  $G$ . Another link was proved by Las Vergnas [37] that  $Z(H; 1, 1, 2) = 2T(G; 3, 3)$  for any plane graph  $G$  with medial graph  $H$ .

\*Department of Computer Sciences, University of Wisconsin-Madison. Supported by NSF CCF-1714275. [jyc@cs.wisc.edu](mailto:jyc@cs.wisc.edu)

<sup>†</sup>Department of Computer Sciences, University of Wisconsin-Madison. Supported by NSF CCF-1714275. [tl@cs.wisc.edu](mailto:tl@cs.wisc.edu)

<sup>‡</sup>ITCS, Shanghai University of Finance and Economics. [lu.pinyan@mail.shufe.edu.cn](mailto:lu.pinyan@mail.shufe.edu.cn)

<sup>1</sup>This is often assumed in physics. From Baxter’s book [2]: “These ensure that on the square lattice the model is unchanged by reversing all arrows, which one would expect to be the situation for a model in zero external electric field. Thus this is a ‘zero-field’ model which includes the ice, KDP and F models as special cases.”

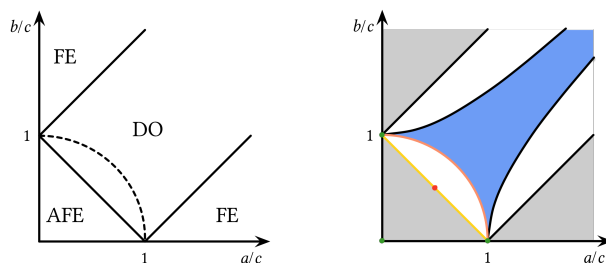
Recently, the exact computational complexity of the six-vertex model has been investigated. This is studied in the context of a classification program for the complexity of counting problems, where the six-vertex model serves as important basic cases for Holant problems defined by not necessarily symmetric constraint functions [4, 3]. It is shown that there are some surprising P-time computable settings, however most occur due to nontrivial cancellations. Under our parameterization of  $a, b, c$  being nonnegative (as is the case in the classical setting), the only P-time (exactly) computable cases are: (1) two of  $a, b, c$  are zero or (2) one of  $a, b, c$  is zero and the other two are equal. Evaluation at any other point for a general graph is #P-hard. On planar graphs it is also P-time computable for parameter settings  $(a, b, c)$  that satisfy: (1)  $c^2 = a^2 + b^2$  or (2) one of  $a, b$  is zero. All other non-trivial P-time computable cases require cancellations (for real or complex parameters  $(a, b, c)$ ) and do not apply for nonnegative  $a, b, c$ . Mihail and Winkler first proved that computing the number of unweighted Eulerian orientations is #P-complete over general graphs [27]. Huang and Lu proved that it remains #P-complete for even degree regular (but not necessarily planar) graphs [13]. Guo and Williams improved it to planar 4-regular graphs [12]. The latter is equivalent to computing the partition function of the six-vertex model on planar graphs with the parameter setting  $(1, 1, 1)$ .

In terms of approximate complexity, results are limited. To our best knowledge, there are only a very few papers that relate to the approximate complexity of the six-vertex model, and they are all on *unweighted* Eulerian orientations. Mihail and Winkler's pioneering work [27] gave the first *fully polynomial randomized approximation scheme (FPRAS)* for the number of Eulerian orientations on a general graph. Luby, Randall, and Sinclair presented an elegant proof of the rapid mixing of a Markov chain that leads to a *fully polynomial almost uniform sampler (FPAUS)* for Eulerian orientations on any region of the Cartesian lattice with fixed boundaries [25]. Randall and Tetali [31] used a comparison technique to prove the single-site Glauber dynamics is rapidly mixing on the same lattice graph, by relating this Markov chain to the Luby-Randall-Sinclair chain. Goldberg, Martin, and Paterson [11] further extended above techniques to prove that the single-site Glauber dynamics is rapidly mixing for the free-boundary case on rectangular regions of the Cartesian lattice. All known results on approximate complexity for the six-vertex model are for the unweighted case, which is the single point  $(1, 1, 1)$  in the parameter space (see Figure 2).

In this paper we initiate a study toward a classifi-

cation of the approximate complexity of the six-vertex model in terms of the parameters. Our results conform to phase transitions in physics.

Here we briefly describe the phenomenon of phase transition of the zero-field six-vertex model (see Baxter's book [2] for more details). On the square lattice in the thermodynamic limit: (1) When  $a > b + c$  (FE: ferroelectric phase) any finite region tends to be frozen into one of the two configurations where either all arrows point up or to the right (Figure 1-1), or all point down or to the left (Figure 1-2). (2) Symmetrically when  $b > a + c$  (also FE) all arrows point down or to the right (Figure 1-3), or all point up or to the left (Figure 1-4). (3) When  $c > a + b$  (AFE: anti-ferroelectric phase) configurations in Figure 1-5 and Figure 1-6 alternate. (4) When  $c < a + b$ ,  $b < a + c$ , and  $a < b + c$ , the system is disordered (DO: disordered phase) in the sense that all correlations decay to zero with increasing distance; in particular on the dashed curve  $c^2 = a^2 + b^2$  the model can be solved by Pfaffians exactly [8], and the correlations decay inverse polynomially, rather than exponentially, in distance. See Figure 2a.



(a) Phase diagram of the six-vertex model. (b) Complexity diagram of the six-vertex model.

Figure 2

In Figure 2b we have a corresponding complexity landscape, its main points are stated in:

**THEOREM 1.1.** *There is an FPRAS for  $Z(G; a, b, c)$  if  $a^2 \leq b^2 + c^2$ ,  $b^2 \leq a^2 + c^2$ , and  $c^2 \leq a^2 + b^2$  (the blue region). There is no FPRAS for  $Z(G; a, b, c)$  if  $a > b + c$  or  $b > a + c$  or  $c > a + b$  (the grey region), unless  $RP = NP$ .*

We obtain our FPRAS for  $Z(G; a, b, c)$  by designing a Markov chain and proving that it is rapidly mixing. The Markov chain is based on the *directed-loop algorithm*. This directed-loop algorithm is invented by Rahman and Stillinger [30] and is widely adopted in the literature (e.g., [38, 1, 35]). The transitions of this algorithm are composed of creating, shifting, and merging

of two “defects” on the edges. This is similar to *the worm process* introduced in [29] for the Ising model (see also [17]). Note that Markov chains that stay within the set of all Eulerian orientations, such as *Glauber dynamics*, are not irreducible for nonplanar 4-regular graphs (e.g. a torus). Therefore, introducing “defects” on the edges, i.e., considering “near-Eulerian” orientations, is indispensable. Moreover, the defects introduced in the directed-loop algorithm depict the *Bjerrum defects* that are observed to happen in real ice [1]. From this perspective, it would be rather artificial to insist that our Markov chain stay “inside” the set of Eulerian orientations, even in cases where such a chain is irreducible. There is no physical reason not to consider a wider variety, nor a mathematical one—as we shall show in this paper that the first provable rapidly mixing Markov chain for a wider parameter space is based on a state space going beyond the set of Eulerian orientations. We give a formal description of the directed-loop algorithm in Section 4. The rapid mixing of this Markov chain is proved by bounding the *conductance* via a *flow argument* [16, 6, 32, 15]. The crucial ingredient in this proof is the closure properties we demonstrate in Section 3.

Our FPRAS result is actually stronger in that the FPRAS works even if different constraint functions from the blue region are assigned at different vertices. The blue region is a proper subset of the disordered phase. The point  $(1, 1, 1)$  is contained in this region, which is the only previously known approximable case. The hardness part (the grey region) coincides with the FE/AFE phases. The three green points together with a point at infinity  $((a, b, c) = (1, 1, 0))$  are exactly P-time computable. All parameters belonging to the two axes  $(a = 0$  and  $b = 0)$  and the orange curve  $c^2 = a^2 + b^2$  are exactly P-time computable on planar graphs. Computing for the six-vertex model at  $(1/2, 1/2, 1)$  (the red point) is equivalent to evaluating the Tutte polynomial  $T(G; 3, 3)$  on planar graphs. Note that any 4-regular plane graph  $H$  is the medial graph of some plane graph  $G$ . The approximation complexity for the white region is unknown.

More structurally, we show that there is a fundamental difference in the behavior on the two sides separated by the phase transition threshold, in terms of closure properties. We use the term *a 4-ary construction* for a 4-regular graph  $\Gamma$  having 4 “external” edges, and consider all configurations on the edges of  $\Gamma$  where every vertex satisfies the ice rule and the arrow reversal symmetry. It turns out that this  $\Gamma$  defines a constraint function of arity 4 that also satisfies the ice rule and the arrow reversal symmetry. If we imagine the graph  $\Gamma$ , except the 4 external edges, is shrunken to a single point, then a 4-ary construction can be viewed as a virtual

vertex with the six-vertex model parameter  $(a', b', c')$  for some  $a', b', c'$ .

In Theorem 3.1 of Section 3, we prove that the set of 4-ary constraint functions lying in the combined region of blue and white (this is the same as the DO region in Figure 2a) is closed under 4-ary constructions. In Theorem 3.2 we prove that the set of 4-ary constraint functions lying on the yellow line (phase transition threshold for AFE and DO) is closed under *planar* 4-ary constructions.

Theorem 3.1 is important not only for its revelation of a structural difference between parameter settings of the six-vertex model on the two sides of the phase transition threshold, but also for its crucial role in giving an FPRAS in Section 4. It is used to upper bound the ratio of near-Eulerian orientations over Eulerian orientations (valid six-vertex configurations). By Lemma 4.1, this shows that the directed-loop algorithm is rapidly mixing. Also, we use Theorem 3.1 to approximately sample the valid six-vertex configurations, which is necessary for our FPRAS to work.

Our FPRAS also has implications for counting weighted sum of directed Eulerian partitions (partition of edges of  $G$  into directed edge-disjoint circuits). A special case is an FPRAS for this weighted sum when the weight of  $\dashv$  is at least  $\sqrt{2} - 1$  (more on the connection between directed Eulerian partitions and the three types of pairings  $\swarrow$ ,  $\nearrow$ , and  $\dashv$  can be found in Section 3).

The NP-hardness of approximation in the grey region (coincide with the ferroelectric/anti-ferroelectric phases) is given by an approximation-preserving reduction from computing the maximum independent set on 3-regular graphs. These are the first inapproximability results for the six-vertex model on general 4-regular graphs.

## 2 Preliminaries

### 2.1 The Six-Vertex Model

We will present the six-vertex model as follows: For any 4-regular graph  $G = (V, E)$ , let  $G' = (U_E, U_V, E')$  be its edge-vertex incidence graph.  $G'$  is a bipartite graph. A configuration of the six-vertex model on  $G$  is an *edge 2-coloring* on  $G'$ , namely  $\sigma : E' \rightarrow \{0, 1\}$ . We model an orientation of edges  $e \in E$  by requiring “one-0 one-1” for the two edges incident to each vertex  $u_e \in U_E$ ; we model the ice rule (2-in-2-out) of  $G$  on all  $v \in V$  by requiring “two-0 two-1” for the four edges incident to each vertex  $u_v \in U_V$  (and the constraint function can have different weights depending on which two edges have 0). We say an orientation on edge  $e = \{w, v\} \in E$  is going out  $w$  and into  $v$  in  $G$  if the edge  $(u_e, u_w) \in E'$  in  $G'$  takes value 1 (and  $(u_e, u_v) \in E'$  takes value 0).

The “one-0 one-1” requirement on the two edges incident to a vertex in  $U_E$  is denoted by  $(\neq_2)$ . A 4-ary constraint function  $f$  can take  $2^4$  values depending on the input, which can be listed in a matrix

$$M(f) = \begin{bmatrix} f_{0000} & f_{0010} & f_{0001} & f_{0011} \\ f_{0100} & f_{0110} & f_{0101} & f_{0111} \\ f_{1000} & f_{1010} & f_{1001} & f_{1011} \\ f_{1100} & f_{1110} & f_{1101} & f_{1111} \end{bmatrix}. \text{ Call this matrix the}$$

constraint matrix of  $f$ . For the six-vertex model satisfying the ice rule and arrow reversal symmetry, the constraint function  $f$  at a vertex  $v \in U_V$  in  $G'$  has the form  $M(f) = \begin{bmatrix} 0 & 0 & 0 & a \\ 0 & b & c & 0 \\ 0 & c & b & 0 \\ a & 0 & 0 & 0 \end{bmatrix}$ , if we locally index the left, down, right, and up edges incident to  $v$  by 1, 2, 3, and 4, respectively according to Figure 1. Thus computing the partition function  $Z(G; a, b, c)$  is equivalent to evaluating

$$Z'(G'; f) := \sum_{\sigma: E' \rightarrow \{0,1\}} \prod_{v \in U_E} (\neq_2)(\sigma|_{E'(v)}) \prod_{v \in U_V} f(\sigma|_{E'(v)}).$$

When it does not cause confusion, we say a vertex (in  $G$ , although strictly it should be in  $G'$ ) in the six-vertex model with parameters  $(a, b, c)$  has the constraint function  $f$  with  $M(f) = \begin{bmatrix} & & & a \\ & b & c & \\ & c & b & \\ a & & & \end{bmatrix}$ . Also, we write the partition function  $Z(a, b, c)$  as  $Z(f)$  and denote by  $Z(\mathcal{F})$  when the constraint functions come from a set  $\mathcal{F}$ . For convenience in presenting our theorems and proofs, we adopt the following notations assuming  $a, b, c \in \mathbb{R}^+$ .

- $\mathcal{F}_{\leq 2} := \{f \mid a^2 \leq b^2 + c^2, b^2 \leq a^2 + c^2, c^2 \leq a^2 + b^2\}$ ;
- $\mathcal{F}_{\leq} := \{f \mid a \leq b + c, b \leq a + c, c \leq a + b\}$ ;
- $\mathcal{F}_= := \{f \mid c = a + b\}$ ;
- $\mathcal{F}_{>} := \{f \mid a > b + c \text{ or } b > a + c \text{ or } c > a + b \text{ where } a, b, c > 0\}$ .

REMARK 2.1.  $\mathcal{F}_{\leq 2} \subset \mathcal{F}_{\leq}$ .

**2.2 Approximation Algorithms** If a counting problem is #P-hard, we may still hope that the problem can be approximated. Suppose  $f : \Sigma^* \rightarrow \mathbb{R}$  is a function mapping problem instances to real numbers. A fully polynomial randomized approximation scheme (FPRAS) [20] for a problem is a randomized algorithm that takes as input an instance  $x$  and  $\varepsilon > 0$ , running in time polynomial in  $n$  (the input length) and  $\varepsilon^{-1}$ , and outputs a number  $Y$  (a random variable) such that

$$\Pr [(1 - \varepsilon)f(x) \leq Y \leq (1 + \varepsilon)f(x)] \geq \frac{3}{4}.$$

### 3 Closure Properties

**THEOREM 3.1.** Consider a 4-ary construction using constraint functions from  $\mathcal{F}_{\leq}$ . Let  $f$  be the resulting constraint function of the 4-ary construction. Then  $f \in \mathcal{F}_{\leq}$ . In other words, the set of constraint functions in  $\mathcal{F}_{\leq}$  is closed under 4-ary constructions.

**THEOREM 3.2.** The set of constraint functions in  $\mathcal{F}_=$  is closed under 4-ary plane constructions.

Before proving Theorem 3.1 and Theorem 3.2, we introduce another view of the six-vertex model. A valid configuration in the six-vertex model, i.e. a weighted Eulerian orientation, can also be viewed as a combination of weighted directed Eulerian partitions. An Eulerian partition of a graph  $G$  is a partition of the edges of  $G$  into edge-disjoint circuits (in which vertices may repeat whereas edges cannot). A directed Eulerian partition is an Eulerian partition where every edge-disjoint circuit takes one of the two cyclic orientations. Let  $G = (V, E)$  be a 4-regular graph and  $v$  be a vertex of  $G$ . Let  $e_1, e_2, e_3, e_4$  be the four edges incident to  $v$ . A pairing  $\varrho$  at  $v$  is a partition of  $\{e_1, e_2, e_3, e_4\}$  into pairs. There are exactly three distinct pairings at  $v$  (Figure 3) which we denote by three special symbols:  $\curvearrowright, \curvearrowleft, \vdash$ , respectively. An Eulerian partition of  $G$  can be uniquely determined by a family of pairings  $\varphi = \{\varrho_v\}_{v \in V}$ , where  $\varrho_v \in \{\curvearrowright, \curvearrowleft, \vdash\}$  is a pairing at  $v$ —once the pairing at each vertex is fixed, then the two edges paired together at each vertex is also adjacent in the same circuit.

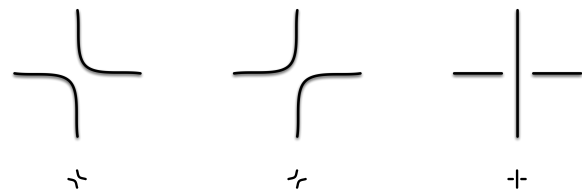


Figure 3: Pairings at a degree 4 vertex.

For any vertex  $v$  in a valid configuration  $\tau$  of the six-vertex model (where ice rule is satisfied), incoming edges can be paired with outgoing edges in exactly two ways, corresponding to two of the three pairings at  $v$ . For example, the configuration in Figure 1-1 of the six-vertex model has two underlying pairings,  $\curvearrowleft$  and  $\vdash$ . Therefore,  $\tau$  can be decomposed into  $2^{|V|}$  distinct directed Eulerian partitions denoted by  $\Phi(\tau)$ . Since no two Eulerian orientations share one directed Eulerian partition and every directed Eulerian partition corresponds to a particular Eulerian orientation, the map from six-vertex configurations to directed Eulerian partitions is 1-to- $2^{|V|}$ , non-overlapping, and surjective. Define  $w$  to be a function assigning a weight to every pairing at every vertex and let the weight  $\tilde{w}(\varphi)$  of an Eulerian partition  $\varphi$ , undirected or directed, be the product of weights at each vertex. In particular, when  $w$  is defined such that

$$\begin{cases} w(\curvearrowright) = \frac{-a+b+c}{2} \\ w(\curvearrowleft) = \frac{a-b+c}{2} \\ w(\vdash) = \frac{a+b-c}{2} \end{cases}, \text{ or equivalently } \begin{cases} a = w(\curvearrowleft) + w(\vdash) \\ b = w(\curvearrowright) + w(\vdash) \\ c = w(\curvearrowright) + w(\curvearrowleft) \end{cases}, \text{ for ev-}$$

ery vertex with constraint matrix  $\begin{bmatrix} & & & a \\ & b & c & \\ & c & b & \\ a & & & \end{bmatrix}$ , then the

weight of a six-vertex model configuration  $\tau$  is equal to  $\sum_{\varphi \in \Phi(\tau)} \tilde{w}(\varphi)$ , by expressing a product of sums as a sum of products.

The connection between Eulerian orientations and Eulerian partitions on 4-regular graphs has been explored in particular parameter settings for the six-vertex model. Las Vergnas [37] demonstrated a special case for plane graphs: the number of directed *non-intersecting* Eulerian partitions is equal to the number of Eulerian orientations with weight 2 on every *saddle* configuration (Figure 1-5 1-6), which is the six-vertex model at  $(1, 1, 2)$ . Jaeger [14] proposed a graph polynomial called *transition polynomial* as a generalization of weighted Eulerian partitions, and related it with weighted Eulerian orientations. The idea of unweighted directed Eulerian partitions was implicitly used in Mihail and Winkler's paper [27] to approximate the number of unweighted Eulerian orientations, where they also adopted the notion of *pairings*. Here we give a general correspondence between weighted Eulerian orientations and weighted Eulerian partitions for the six-vertex model in the proof of Theorem 3.1 and Theorem 3.2. In particular we establish a weight-preserving 1-to- $2^{|V|}$ , non-overlapping, and surjective mapping for Eulerian orientations in  $\mathcal{F}_{\leq}$  and nonnegatively weighted Eulerian partitions. This "quantum graph" perspective is at the heart of the proof in this paper.

*Proof.* [Proof of Theorem 3.1] For the constraint function  $f$  of a 4-ary construction using vertices with constraint functions in  $\mathcal{F}_{\leq}$  (Figure 4a), we first show that

$$\text{its constraint matrix must be of the form } \begin{bmatrix} & b' & c' & a' \\ a' & & c' & b' \end{bmatrix}.$$

This is to say that the ice rule and the arrow reversal symmetry are still satisfied. First,  $f$  still obeys the ice rule, i.e. it cannot take nonzero values on inputs with Hamming weight not 2. Including the dangling edges, every vertex has exactly two incoming edges and two outgoing edges. Thus if we sum the in-degrees over all vertices, it must equal to the sum of out-degrees over all vertices. Every internal edge contributes exactly 1 to each sum. Thus the number of incoming dangling edges is equal to the number of outgoing dangling edges, which must be 2 each since they sum to 4. Second,  $f$  still satisfies arrow reversal symmetry. For any valid orientation of edges in the 4-ary construction contributing a term to  $f(x)$ , reversing the orientations on all edges has the same contribution to  $f(\bar{x})$ , because the constraint function on each vertex of degree 4 satisfies the arrow reversal symmetry.

The notion of Eulerian partitions previously used for graphs (without external edges) can also be defined for 4-ary constructions. An *Eulerian partition* for a

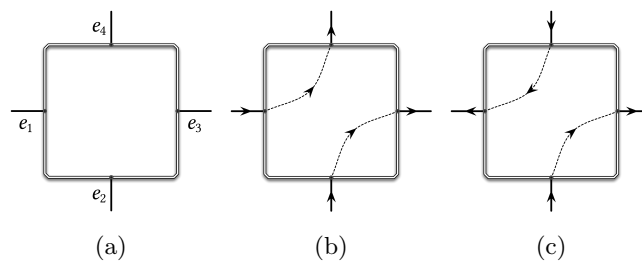


Figure 4: A 4-ary construction using vertices with constraint function in  $\mathcal{F}_{\leq}$ .

*4-ary construction*  $g$  is a partition of the edges in  $g$  into edge-disjoint circuits and exactly two *trails* (walks with no repeated edges) whose ends are exactly the four dangling edges. The weight  $\tilde{w}$  of such an Eulerian partition  $\varphi$  can be similarly defined. Set  $w$  such

$$\text{that } \begin{cases} w(\curvearrowright) = \frac{-a+b+c}{2} \\ w(\curvearrowleft) = \frac{a-b+c}{2} \\ w(\dashv) = \frac{a+b-c}{2} \end{cases}, \text{ or equivalently } \begin{cases} a = w(\curvearrowright) + w(\dashv) \\ b = w(\curvearrowleft) + w(\dashv) \\ c = w(\curvearrowright) + w(\curvearrowleft) \end{cases}.$$

Observe that if a vertex has a constraint function  $f \in \mathcal{F}_{\leq}$ , then the weight of every pairing is *nonnegative*, and the weight of any directed Eulerian partition of a graph/4-ary construction comprised of such vertices is also *nonnegative*.

Under the six-vertex model, for any specific configuration  $\tau$  of the 4-ary construction with constraint function  $f$  that contributes a nonzero factor to  $f(0011)$  when  $e_1, e_2$  go in and  $e_3, e_4$  go out, it can be viewed as a weighted sum of directed Eulerian partitions  $\Phi(\tau)$ . For every Eulerian partition  $\varphi \in \Phi(\tau)$ , the two directed trails are either  $\{e_1 \rightsquigarrow e_4, e_2 \rightsquigarrow e_3\}$  (Figure 4b) or  $\{e_1 \rightsquigarrow e_3, e_2 \rightsquigarrow e_4\}$ . Denote by  $\Phi_{0011, \curvearrowright}$  the set of directed Eulerian partitions (distributed in potentially many different six-vertex configurations), each of which has directed trails  $\{e_1 \rightsquigarrow e_4, e_2 \rightsquigarrow e_3\}$ ; denote by  $\Phi_{0011, \dashv}$  the set of directed Eulerian partitions, each of which has directed trails  $\{e_1 \rightsquigarrow e_3, e_2 \rightsquigarrow e_4\}$ . In terms of directed Eulerian partitions of the 4-ary construction,  $f(0011)$  can be seen as the weighted sum of elements from two disjoint sets  $\Phi_{0011, \curvearrowright}$  and  $\Phi_{0011, \dashv}$ . Defining the weight of a set  $\Phi$  of directed Eulerian partitions by  $W(\Phi) = \sum_{\varphi \in \Phi} \tilde{w}(\varphi)$  yields  $f(0011) = W(\Phi_{0011, \curvearrowright}) + W(\Phi_{0011, \dashv})$ , and similarly  $f(1100) = W(\Phi_{1100, \curvearrowright}) + W(\Phi_{1100, \dashv})$ . Note that there is a bijective weight-preserving map between  $\Phi_{0011, \curvearrowright}$  and  $\Phi_{1100, \curvearrowright}$  by reversing the direction of every circuit and trail of an Eulerian partition. Thus,  $W(\Phi_{0011, \curvearrowright}) = W(\Phi_{1100, \curvearrowright})$  and similarly  $W(\Phi_{0011, \dashv}) = W(\Phi_{1100, \dashv})$ . Consequently,  $f(0011) = f(1100)$ ,  $f(0110) = f(1001)$ , and  $f(0101) = f(1010)$ .

An important observation is that for each Eulerian

partition in  $\Phi_{0011, \mathcal{J}_r}$ , if we only reverse the trail from  $e_1 \rightsquigarrow e_4$  to  $e_4 \rightsquigarrow e_1$  and keep the directions on all circuits and the other trail unchanged, this Eulerian partition has the same weight but now lies in  $\Phi_{1010, \mathcal{J}_r}$  (Figure 4c). This is because at every vertex  $v$ , reversing any orientation of a branch of the given pairing  $\varrho_v \in \{\curvearrowright, \curvearrowleft, \dashv\}$  does not change the value  $w(\varrho_v)$ . In this way, we set up a one-to-one weight-preserving map between  $\Phi_{0011, \mathcal{J}_r}$  and  $\Phi_{1010, \mathcal{J}_r}$ , i.e.  $W(\Phi_{0011, \mathcal{J}_r}) = W(\Phi_{1010, \mathcal{J}_r})$ . Combining the result in the last paragraph, we can write

- $W(\mathcal{J}_r) = W(\Phi_{0011, \mathcal{J}_r}) = W(\Phi_{1100, \mathcal{J}_r}) = W(\Phi_{0101, \mathcal{J}_r}) = W(\Phi_{1010, \mathcal{J}_r})$ ;
- $W(\curvearrowright) = W(\Phi_{0110, \curvearrowright}) = W(\Phi_{1001, \curvearrowright}) = W(\Phi_{0101, \curvearrowright}) = W(\Phi_{1010, \curvearrowleft})$ ;
- $W(\dashv) = W(\Phi_{0011, \dashv}) = W(\Phi_{1100, \dashv}) = W(\Phi_{0110, \dashv}) = W(\Phi_{1001, \dashv})$ .

Consequently, we have  $\begin{cases} a' = W(\mathcal{J}_r) + W(\dashv) \\ b' = W(\curvearrowright) + W(\dashv) \\ c' = W(\curvearrowright) + W(\mathcal{J}_r) \end{cases} \cdot W(\mathcal{J}_r)$ ,

$W(\curvearrowright)$ , and  $W(\dashv)$  are all nonnegative due to the fact that the weight of every directed Eulerian partition has a nonnegative weight. Therefore,  $a' \leq b' + c'$ ,  $b' \leq a' + c'$ , and  $c' \leq a' + b'$ . This is to say,  $f \in \mathcal{F}_{\leq}$ .

*Proof.* [Proof of Theorem 3.2] Inheriting the notations from the above proof, we have  $w(\dashv) = 0$  when  $c = a + b$  for each vertex, which is to say no “crossing” can be made at any vertex in any Eulerian partition. Due to planarity, a trail  $e_1 \rightsquigarrow e_3$  must cross a trail  $e_2 \rightsquigarrow e_4$  at a vertex, thus  $W(\dashv) = W(\Phi_{0011, \dashv}) = 0$ . Therefore,  $c' = a' + b'$ .

**REMARK 3.1.** *Theorem 3.1 is important not only because it reveals a structural difference between parameter settings of the six-vertex model lying on the two sides of the phase transition threshold, but also for its crucial role in proving Corollary 4.1 which helps us upper bound the mixing time of the directed-loop algorithm and lower bound the proportion of valid six-vertex model configurations in the state space so that approximately counting via sampling [19] leads to an FPRAS.*

## 4 FPRAS

In this section we prove the following theorem.

**THEOREM 4.1.** *There is an FPRAS for computing  $Z(\mathcal{F}_{\leq 2})$ .*

For simplicity we prove Theorem 4.1 only for the case where all constraint functions of arity 4 are from a fixed finite subset  $\mathcal{F} \subset \mathcal{F}_{\leq 2}$ , i.e., we show that there is an FPRAS for computing  $Z(\mathcal{F})$ . With some care the more general statement in Theorem 4.1 can also be proved.

We use the common approach to approximate counting via almost uniform sampling [19] using a rapidly mixing Markov chain [16, 6, 32, 15]. The Markov chain is the widely-used directed-loop algorithm [30, 38, 1, 35] whose transitions are composed of creating, shifting, and merging of two “defects” on the edges. Some examples of the states in the directed-loop algorithm are shown in Figure 5 where the state in Figure 5a is an Eulerian orientation and the state in Figure 5b and the state in Figure 5c are “near-Eulerian” orientations with exactly two “defects”. Some typical moves in the directed-loop algorithm are as follows: the transition from the state in Figure 5a to the state in Figure 5b creates two defects; the transition from the state in Figure 5b to the state in Figure 5a merges two defects; the transitions between Figure 5b and Figure 5c shift one of the defects.

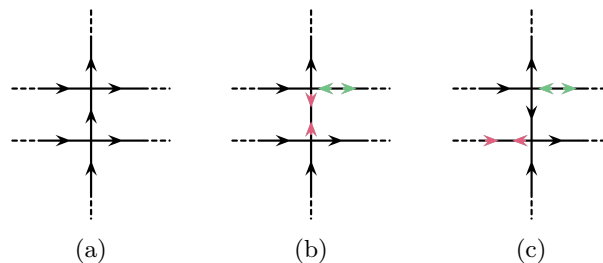


Figure 5: Examples of the states in the directed-loop algorithm.

Although the directed-loop algorithm  $\mathcal{MC}$  runs on the Eulerian orientations of a 4-regular graph  $G$ , it is formally defined and analyzed using the edge-vertex incidence graph  $G'$  of  $G$ , introduced in Section 2. Let  $G' = (V, U, E)$  be the edge-vertex incidence graph of  $G$ , an instance of  $Z(\mathcal{F}_{\leq 2})$ . Each vertex in  $V$  is assigned  $(\neq_2)$ ; each vertex  $u \in U$  is assigned a constraint function  $f_u \in \mathcal{F}_{\leq 2}$ . An assignment  $\sigma$  assigns a value in  $\{0, 1\}$  to each edge  $e \in E$ . The state space of  $\mathcal{MC}$  is  $\Omega = \Omega_0 \cup \Omega_2$ , which consists of “perfect” or “near-perfect” assignments to  $E$ , defined as follows: All assignments satisfy the “two-0 two-1” ice rule at every vertex  $u \in U$  of degree 4. We also insist that all assignments satisfy the “one-0 one-1” at every  $v \in V$  with possibly exactly two exceptions. Assignments in  $\Omega_0$  have no exceptions, and are “perfect” (corresponding to the Eulerian orientations in  $G$ ). Assignments in  $\Omega_2$  have exactly two exceptions, and are “near-perfect” (corresponding to the near-Eulerian orientations in  $G$ ). Thus any  $\sigma \in \Omega_0$  satisfies all  $(\neq_2)$  on  $V$ , and any  $\sigma \in \Omega_2$  satisfies all  $(\neq_2)$  on  $V - \{v', v''\}$  for some two vertices  $v', v'' \in V$  where it satisfies  $(=_2)$  (which outputs 1 on inputs 00, 11 and outputs 0 on 01, 10).

For any assignment  $\sigma \in \Omega$  and any subset

$S \subseteq \Omega$ , define the *weight* function  $\mathcal{W}$  by  $\mathcal{W}(\sigma) = \prod_{u \in U} f_u(\sigma|_{E(u)})$  and  $\mathcal{Z}(S) = \sum_{\sigma \in S} \mathcal{W}(\sigma)$ . Then the *Gibbs measure* for  $\Omega$  is defined by  $\pi(\sigma) = \frac{\mathcal{W}(\sigma)}{\mathcal{Z}(\Omega)}$ , assuming  $\mathcal{Z}(\Omega) > 0$ . Observe that if a state  $\sigma \in \Omega_2$  assigns 00 to both edges incident to  $v' \in V$  (satisfying  $(=)_2$  at  $v'$ ) then it must assign 11 to both edges incident to  $v'' \in V$ , and vice versa. Indeed, having 00 at  $v'$  models the fact that  $v'$  has two arrows going out (to degree-4 vertices in  $U$ ). To maintain the property that the number of incoming arrows is equal to the number of outgoing arrows everywhere else,  $v''$  must have two arrows coming in, which is equivalent to having 11 at  $v''$  in the edge 2-coloring model of the edge-vertex incidence graph. An example state is shown in Figure 7a.

Transitions in  $\mathcal{MC}$  are comprised of three types of moves. Suppose  $\sigma \in \Omega_0$ . An  $\Omega_0$ -to- $\Omega_2$  move from  $\sigma$  takes a degree 4 vertex  $u \in U$  and two incident edges  $e' = (v', u), e'' = (v'', u) \in V \times U$  satisfying  $\{\sigma(e'), \sigma(e'')\} = \{0, 1\}$ , and changes it to  $\sigma_2 \in \Omega_2$  which flips both  $\sigma(e')$  and  $\sigma(e'')$ . The effect is that we still have  $\{\sigma_2(e'), \sigma_2(e'')\} = \{0, 1\}$ , but at  $v'$  and  $v''$ ,  $\sigma_2$  satisfies  $(=)_2$  instead. An  $\Omega_2$ -to- $\Omega_0$  move is the opposite. An  $\Omega_2$ -to- $\Omega_2$  move is, intuitively, to *shift* one  $(=)_2$  from one vertex  $v' \in V$  to another  $v^* \in V$ , where for some  $u \in U$ ,  $v'$  and  $v^*$  are both incident to  $u$  and the “two-0 two-1” rule at  $u$  is preserved. Formally, let  $\sigma \in \Omega_2$  be a near-perfect assignment with  $v', v'' \in V$  being the two exceptional vertices (i.e.,  $\sigma$  satisfies  $(=)_2$  at  $v'$  and  $v''$ ). Let  $v^* \in V - \{v', v''\}$  be such that for some  $u \in U$ , both  $e' = (v', u), e^* = (v^*, u) \in E$ , and  $\{\sigma(e'), \sigma(e^*)\} = \{0, 1\}$ . Then an  $\Omega_2$ -to- $\Omega_2$  move changes  $\sigma$  to  $\sigma^*$  by flipping both  $\sigma(e')$  and  $\sigma(e^*)$ . The effect is that we still have  $\{\sigma^*(e'), \sigma^*(e^*)\} = \{0, 1\}$ , but  $\sigma^*$  satisfies  $(\neq)_2$  at  $v'$  and  $(=)_2$  at  $v^*$ . Note that  $\sigma^*$  continues to satisfy  $(=)_2$  at  $v''$ .

The above describes a symmetric binary relation *neighbor* ( $\sim$ ) on  $\Omega$ . No two states in  $\Omega_0$  are neighbors. Set  $n = |U|$ . The number of neighbors of a  $\Omega_0$ -state is at most  $4n$  (by first picking a vertex and then picking an “in-out” pair of edges incident to this vertex) and the number of neighbors of a  $\Omega_2$ -state is at most a constant. The transition probabilities  $P(\cdot, \cdot)$  of  $\mathcal{MC}$  are *Metropolis* moves between neighboring states:

$$P(\sigma_1, \sigma_2) = \begin{cases} \frac{1}{8n} \min\left(1, \frac{\pi(\sigma_2)}{\pi(\sigma_1)}\right) & \text{if } \sigma_2 \sim \sigma_1; \\ 1 - \frac{1}{8n} \sum_{\sigma' \sim \sigma_1} \min\left(1, \frac{\pi(\sigma')}{\pi(\sigma_1)}\right) & \text{if } \sigma_1 = \sigma_2; \\ 0 & \text{otherwise.} \end{cases}$$

$\mathcal{MC}$  is aperiodic due to the “lazy” movement; one can verify that  $\mathcal{MC}$  is irreducible by creating, shifting, and merging of a pair of  $(=)_2$ 's; as the transitions are Metropolis moves, detailed balance conditions are satisfied with regard to  $\pi$ . By results from [16, 32], such a Markov chain is rapidly mixing if there is a *flow* whose

congestion can be bounded by a polynomial in  $n$ .

LEMMA 4.1. *Assume  $\mathcal{Z}(\Omega_0) > 0$ . There is a flow on  $\Omega$  with congestion at most  $O\left(n^2 \left(\frac{\mathcal{Z}(\Omega)}{\mathcal{Z}(\Omega_0)}\right)^2\right)$ , using paths of length  $O(n)$ .*

*Proof.* The idea is to design a flow  $\mathfrak{F} : \mathcal{P} \rightarrow \mathbb{R}^+$  from  $\Omega_2$  to  $\Omega_0$  which satisfies

$$\sum_{p \in \mathcal{P}_{\sigma_2 \sigma_0}} \mathfrak{F}(p) = \pi(\sigma_2)\pi(\sigma_0), \quad \text{for all } \sigma_2 \in \Omega_2, \sigma_0 \in \Omega_0,$$

where  $\mathcal{P}_{\sigma_2 \sigma_0}$  is defined to be a set of simple directed paths from  $\sigma_2$  to  $\sigma_0$  in  $\mathcal{MC}$  and  $\mathcal{P} = \bigcup_{\sigma_2 \in \Omega_2, \sigma_0 \in \Omega_0} \mathcal{P}_{\sigma_2 \sigma_0}$ . Once the congestion of  $\mathfrak{F}$  from  $\Omega_2$  to  $\Omega_0$  is polynomially bounded, so is the flow from  $\Omega_0$  to  $\Omega_2$  by symmetric construction. Moreover, there is a flow from  $\Omega_2$  to  $\Omega_2$  (or from  $\Omega_0$  to  $\Omega_0$ ) whose congestion can also be polynomially bounded by randomly picking an intermediate state in  $\Omega_0$  (or  $\Omega_2$ , respectively). Thus we have a flow on  $\Omega$  with polynomially bounded congestion. This technique has been used in [18, 26]. In the following we show that the congestion of  $\mathfrak{F}$  from  $\Omega_2$  to  $\Omega_0$  is bounded by  $O(n^2 \frac{\mathcal{Z}(\Omega_2)}{\mathcal{Z}(\Omega_0)})$ . Then the bound in the lemma for a flow on  $\Omega$  follows.

To describe the flow  $\mathfrak{F}$ , we first specify the sets of paths that are going to take the flow. In line with the definition of  $\Omega_0$  and  $\Omega_2$ , we define  $\Omega_4$  to be the set of assignments where there are exactly four violations of  $(\neq)_2$  in  $V$ . Let  $\Omega' = \Omega_0 \cup \Omega_2 \cup \Omega_4$ . For  $\sigma, \sigma' \in \Omega'$ , let  $\sigma \oplus \sigma'$  denote the *symmetric difference* (or bitwise XOR), where we view  $\sigma$  and  $\sigma'$  as two bit strings in  $\{0, 1\}^{|E|}$ . This is a 0-1 assignment to the edge set of the edge-vertex incidence graph  $G' = (V, U, E)$  of  $G$ . We also treat  $\sigma \oplus \sigma'$  as an edge subset of  $E$  (corresponding to bit positions having bit 1, where  $\sigma$  and  $\sigma'$  assign opposite values), and this defines an induced subgraph of  $G'$ . Since at every  $u \in U$  of degree 4, the “two-0 two-1” rule is satisfied by both  $\sigma$  and  $\sigma'$ , this induced subgraph has even degree (0, 2, or 4) at every  $u \in U$ .

Denote by  $U_4 \subseteq U$  the degree-4 vertices in  $\sigma \oplus \sigma'$ . Then there are exactly  $2^{|U_4|}$  Eulerian partitions for  $\sigma \oplus \sigma'$ . Recall that an Eulerian partition of  $\sigma \oplus \sigma'$  is uniquely determined by a family of pairings on  $U_4$ . This is a 1-1 correspondence and we will identify the two sets. For any pairing in  $\{\swarrow, \nearrow, \vdash\}$  on a vertex  $u$  with constraint matrix  $M(f_u) = \begin{bmatrix} & b & c \\ a & & \\ c & b & \end{bmatrix}$ , define the weight

$$\text{function } \mathfrak{w} \text{ for pairings as follows, } \begin{cases} \mathfrak{w}(\swarrow) = \frac{-a^2 + b^2 + c^2}{2} \\ \mathfrak{w}(\nearrow) = \frac{a^2 - b^2 + c^2}{2} \\ \mathfrak{w}(\vdash) = \frac{a^2 + b^2 - c^2}{2} \end{cases},$$

or equivalently  $\begin{cases} a^2 = \mathfrak{w}(\nearrow) + \mathfrak{w}(\vdash) \\ b^2 = \mathfrak{w}(\swarrow) + \mathfrak{w}(\vdash) \\ c^2 = \mathfrak{w}(\swarrow) + \mathfrak{w}(\nearrow) \end{cases}$ . Note that when  $f_u \in$

$\mathcal{F}_{<2}$ ,  $\mathfrak{w}$  takes nonnegative values. Let  $\Phi_{\sigma \oplus \sigma'}$  be the set of Eulerian partitions for  $\sigma \oplus \sigma'$ . For  $\varphi \in \Phi_{\sigma \oplus \sigma'}$ , define

$$\mathfrak{W}(\sigma, \sigma', \varphi) := \left( \prod_{u \in U \setminus U_4} f_u(\sigma|_{E(u)}) f_u(\sigma'|_{E(u)}) \right) \left( \prod_{u \in U_4} \mathfrak{w}(\varphi(u)) \right).$$

Then for all distinct  $\sigma, \sigma' \in \Omega'$ , we have

$$\begin{aligned} & \sum_{\varphi \in \Phi_{\sigma \oplus \sigma'}} \mathfrak{W}(\sigma, \sigma', \varphi) \\ &= \sum_{\varphi \in \Phi_{\sigma \oplus \sigma'}} \prod_{u \in U \setminus U_4} f_u(\sigma|_{E(u)}) f_u(\sigma'|_{E(u)}) \prod_{u \in U_4} \mathfrak{w}(\varphi(u)) \\ &= \prod_{u \in U \setminus U_4} f_u(\sigma|_{E(u)}) f_u(\sigma'|_{E(u)}) \sum_{\varphi \in \Phi_{\sigma \oplus \sigma'}} \prod_{u \in U_4} \mathfrak{w}(\varphi(u)) \\ &= \prod_{u \in U \setminus U_4} f_u(\sigma|_{E(u)}) f_u(\sigma'|_{E(u)}) \prod_{u \in U_4} f_u(\sigma|_{E(u)}) f_u(\sigma'|_{E(u)}) \\ &= \prod_{u \in U} f_u(\sigma|_{E(u)}) f_u(\sigma'|_{E(u)}) \\ &= \mathcal{W}(\sigma) \mathcal{W}(\sigma'). \end{aligned}$$

The equality from line 2 to line 3 is due to the following: when the degree (in the induced subgraph  $\sigma \oplus \sigma'$ ) of a vertex  $u \in U$  is 4,  $\sigma$  and  $\sigma'$  must take the same value at  $u$ , since one represents a total reversal of all arrows of another; thus  $f_u(\sigma|_{E(u)}) f_u(\sigma'|_{E(u)})$  is in  $\{a^2, b^2, c^2\}$ . Then

$$\prod_{u \in U_4} f_u(\sigma|_{E(u)}) f_u(\sigma'|_{E(u)}) = \sum_{\varphi \in \Phi_{\sigma \oplus \sigma'}} \prod_{u \in U_4} \mathfrak{w}(\varphi(u))$$

is obtained by using the sum expressions for  $a^2, b^2$  and  $c^2$  in terms of  $\mathfrak{w}(\curvearrowright), \mathfrak{w}(\curvearrowleft),$  and  $\mathfrak{w}(\dashv)$ , and then expressing the product-of-sums as a sum-of-products.

Now we are ready to specify the “paths” which take nonzero flow from  $\sigma_2 \in \Omega_2$  to  $\sigma_0 \in \Omega_0$ . In order to transit from  $\sigma_2$  to  $\sigma_0$ , paths in  $\mathcal{P}_{\sigma_2 \sigma_0}$  go through states in  $\Omega$  that gradually decrease the number of conflicting assignments along trails and circuits in  $\sigma_2 \oplus \sigma_0$ . We first specify a total order on  $E$ , the set of edges of  $G'$ . This induces a total order on circuits by lexicographic order. In the induced subgraph  $\sigma_2 \oplus \sigma_0$ , exactly two vertices in  $V$  have degree 1 (called *endpoints*) and all other vertices have degree 2 or degree 4. The set of paths in  $\mathcal{P}_{\sigma_2 \sigma_0}$  are designed to be in 1-to-1 correspondence with elements in  $\Phi_{\sigma_2 \oplus \sigma_0}$ . Given any family of pairings  $\varphi \in \Phi_{\sigma_2 \oplus \sigma_0}$ , we have a unique decomposition of the induced subgraph  $\sigma_2 \oplus \sigma_0$  as an edge disjoint union of one trail  $[e_1](v_1, e'_1, u_1, e_2, v_2, e'_2, u_2, \dots, e_k, v_k)[e'_k]$  (where  $e_1$  and  $e'_k$  are not part of the trail), and zero or more edge disjoint circuits, which are ordered lexicographically. Here  $v_i \in V$  and  $u_i \in U$ , and we may assume  $\sigma_2(e_1) = \sigma_2(e'_1) = 0, \sigma_2(e_2) = 1, \sigma_2(e'_2) = 0, \dots, \sigma_2(e_k) =$

$\sigma_2(e'_k) = 1$ . So the two exceptional vertices are  $v_1$  and  $v_k$ , where  $\sigma_2$  satisfies  $(=2)$ . The unique path  $p_\varphi$  first “pushes” the  $(=2)$  from  $v_1$ , to  $v_2$ , then to  $v_3, \dots, v_{k-1}$ , and then “merge” at  $v_k$ , arriving at a configuration in  $\Omega_0$ . Then  $p_\varphi$  reverses all arrows on each circuit in lexicographic order, and within each circuit  $C$  it starts at the least edge  $e$  (according to the edge order) and reverses all arrows on  $C$  in the direction defined by the starting cyclic orientation of  $\sigma_2$ . (Technically it flips a pair of incident edges to vertices in  $U$  in each step.) Such paths  $p_\varphi$  are well-defined and are valid paths in  $\mathcal{MC}$  since along any path every state is in  $\Omega = \Omega_0 \cup \Omega_2$  and every move is a valid transition defined in  $\mathcal{MC}$ . With regard to the flow distribution, the flow value put on  $p_\varphi$  is  $\frac{\mathfrak{W}(\sigma_2, \sigma_0, \varphi)}{(\mathcal{Z}(\Omega))^2}$ , making the following hold for all  $\sigma_2 \in \Omega_2, \sigma_0 \in \Omega_0$ :

$$\begin{aligned} \sum_{p_\varphi \in \mathcal{P}_{\sigma_2 \sigma_0}} \mathfrak{F}(p_\varphi) &= \sum_{\varphi \in \Phi_{\sigma_2 \oplus \sigma_0}} \frac{\mathfrak{W}(\sigma_2, \sigma_0, \varphi)}{(\mathcal{Z}(\Omega))^2} \\ &= \frac{\mathcal{W}(\sigma_2) \mathcal{W}(\sigma_0)}{(\mathcal{Z}(\Omega))^2} \\ &= \pi(\sigma_2) \pi(\sigma_0). \end{aligned}$$

Note that in each path, no edge is flipped more than once, so the length is  $O(n)$ . For any transition  $(\sigma', \sigma'')$  where  $\sigma' \neq \sigma''$ , we have  $P(\sigma', \sigma'') = \frac{1}{8n} \min\left(1, \frac{\pi(\sigma'')}{\pi(\sigma')}\right) = \Omega\left(\frac{1}{n}\right)$ , as  $\frac{\pi(\sigma'')}{\pi(\sigma')}$  is a constant. (This is a constant because we have restricted the constraint function  $f_u$  to be from a fixed finite set  $\mathcal{F}$ .) Let  $H_{\sigma'} = \{\sigma_2 \oplus \sigma_0 \mid \sigma_2 \in \Omega_2, \sigma_0 \in \Omega_0, \exists \varphi \in \Phi_{\sigma_2 \oplus \sigma_0} \text{ s.t. } \sigma' \in p_\varphi\}$ . The congestion of  $\mathfrak{F}$  is

$$\begin{aligned} & \max_{\text{transition } (\sigma', \sigma'')} \frac{1}{\pi(\sigma') P(\sigma', \sigma'')} \sum_{\substack{\sigma_2 \in \Omega_2 \\ \sigma_0 \in \Omega_0}} \sum_{\substack{p_\varphi \in \mathcal{P}_{\sigma_2 \sigma_0} \\ p_\varphi \ni (\sigma', \sigma'')}} \frac{\mathfrak{W}(\sigma_2, \sigma_0, \varphi)}{(\mathcal{Z}(\Omega))^2} \\ & \leq \max_{\sigma' \in \Omega} \frac{O(n)}{\mathcal{W}(\sigma') \mathcal{Z}(\Omega)} \sum_{\substack{\sigma_2 \in \Omega_2 \\ \sigma_0 \in \Omega_0}} \sum_{\substack{\varphi \in \Phi_{\sigma_2 \oplus \sigma_0} \\ p_\varphi \ni \sigma'}} \mathfrak{W}(\sigma_2, \sigma_0, \varphi) \\ & = \max_{\sigma' \in \Omega} \frac{O(n)}{\mathcal{W}(\sigma') \mathcal{Z}(\Omega)} \sum_{\sigma_2 \in \Omega_2} \sum_{\eta \in H_{\sigma'}} \sum_{\varphi \in \Phi_\eta} \mathfrak{W}(\sigma_2, \sigma_2 \oplus \eta, \varphi) \\ & = \max_{\sigma' \in \Omega} \frac{O(n)}{\mathcal{W}(\sigma') \mathcal{Z}(\Omega)} \sum_{\eta \in H_{\sigma'}} \sum_{\varphi \in \Phi_\eta} \sum_{\sigma_2 \in \tilde{\Omega}_2} \mathfrak{W}(\sigma_2, \sigma_2 \oplus \eta, \varphi). \end{aligned}$$

On the last line above we exchange the order of summations where  $\tilde{\Omega}_2$  is the set of  $\Omega_2$ -states that are compatible with the symmetric difference  $\eta$  and its Eulerian partition  $\varphi$ . The number of states in  $\tilde{\Omega}_2$  is bounded by the length of the longest path  $O(n)$  because  $\sigma'$  is an intermediate state on a path. Fix any  $\sigma' \in \Omega$ . For any  $\sigma_2 \in \Omega_2$ , and  $\eta \in H_{\sigma'}$  consisting of exactly one connected component with two endpoints of degree 1 and all other vertices having even degree (and zero or

more connected components of even degree vertices), observe that  $\sigma' \oplus \eta \in \Omega'$ . Indeed, if  $\sigma' \in \Omega_0$  then  $\sigma' \oplus \eta \in \Omega_2$ ; if  $\sigma' \in \Omega_2$  then depending on whether  $\sigma'$

- (1) is  $\sigma_2$ , or
- (2) appears in the process of reversing arrows on the trail with two endpoints, or
- (3) appears after reversing arrows on the trail with endpoints,

$\sigma' \oplus \eta$  lies in  $\Omega_0, \Omega_2$ , or  $\Omega_4$ , respectively. For the edges not in  $\eta$ ,  $\sigma'$  agrees with  $\sigma_2$  and  $\sigma_2 \oplus \eta$  as the path  $p_\varphi$  never “touches” them, and so does  $\sigma' \oplus \eta$ . Recall that

$$\mathfrak{W}(\sigma_2, \sigma_2 \oplus \eta, \varphi) = \left( \prod_{u \in U \setminus U_4} f_u(\sigma_2|_{E(u)}) f_u((\sigma_2 \oplus \eta)|_{E(u)}) \right) \left( \prod_{u \in U_4} \mathfrak{w}(\varphi(u)) \right).$$

For every vertex  $u \in U$  that is not in  $\eta$ ,  $f_u$  takes the same value in all  $\sigma_2, \sigma_2 \oplus \eta, \sigma'$ , and  $\sigma' \oplus \eta$ . For every vertex  $u \in U$  that is degree-2 in  $\eta$ , assuming  $M(f_u) = \begin{bmatrix} & b & c & a \\ a & & & \end{bmatrix}$ ,  $f_u(\sigma_2|_{E(u)})$  and  $f_u((\sigma_2 \oplus \eta)|_{E(u)})$  take two different elements in  $\{a, b, c\}$ . Meanwhile,  $f_u(\sigma'|_{E(u)})$  and  $f_u(\sigma' \oplus \eta|_{E(u)})$  also take these two elements (possibly in the opposite order). For example, at the vertex  $u$  shown in Figure 6,  $f_u(\sigma_2|_{E(u)}) = a$  and  $f_u(\sigma_2 \oplus \eta|_{E(u)}) = c$ . The two solid edges are in  $\eta$  and assignments on the two dotted edges are shared by  $\sigma_2$  and  $\sigma_2 \oplus \eta$ , as well as  $\sigma'$  and  $\sigma' \oplus \eta$ . On the path  $p_\varphi$  from  $\sigma_2$  to  $\sigma_2 \oplus \eta$  decided by  $\varphi$ : if  $\sigma'$  appears before reversing the two solid edges, then  $\sigma'$  agrees with  $\sigma_2$  on them ( $f_u(\sigma'|_{E(u)}) = a$ ) and  $\sigma' \oplus \eta$  agrees with  $\sigma_2 \oplus \eta$  on them ( $f_u(\sigma' \oplus \eta|_{E(u)}) = c$ ); if  $\sigma'$  appears after reversing the two solid edges, then  $\sigma'$  agrees with  $\sigma_2 \oplus \eta$  on them ( $f_u(\sigma'|_{E(u)}) = c$ ) and  $\sigma' \oplus \eta$  agrees with  $\sigma_2$  on them ( $f_u(\sigma' \oplus \eta|_{E(u)}) = a$ ). For every vertex  $u \in U$  that is degree-4 in  $\eta$ ,  $\mathfrak{w}(\varphi(u))$  takes the same value in  $\mathfrak{W}(\sigma_2, \sigma_2 \oplus \eta, \varphi)$  and  $\mathfrak{W}(\sigma', \sigma' \oplus \eta, \varphi)$  as the weight only depends on  $\varphi(u)$ , the pairing at  $u$ .

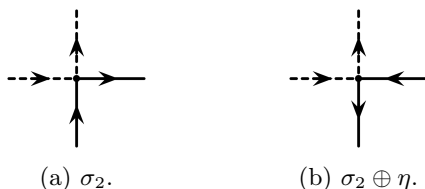


Figure 6

By the above argument, we established that  $\mathfrak{W}(\sigma_2, \sigma_2 \oplus \eta, \varphi) = \mathfrak{W}(\sigma', \sigma' \oplus \eta, \varphi)$ . Therefore, the con-

gestion of  $\mathfrak{F}$  can be bounded by

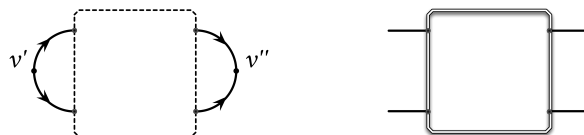
$$\begin{aligned} & \max_{\sigma' \in \Omega} \frac{O(n)}{\mathcal{W}(\sigma') \mathcal{Z}(\Omega)} \sum_{\eta \in H_{\sigma'}} \sum_{\varphi \in \Phi_\eta} \sum_{\sigma_2 \in \tilde{\Omega}_2} \mathfrak{W}(\sigma', \sigma' \oplus \eta, \varphi) \\ & \leq \max_{\sigma' \in \Omega} \frac{O(n^2)}{\mathcal{W}(\sigma') \mathcal{Z}(\Omega)} \sum_{\eta \in H_{\sigma'}} \sum_{\varphi \in \Phi_\eta} \mathfrak{W}(\sigma', \sigma' \oplus \eta, \varphi) \\ & \leq \max_{\sigma' \in \Omega} \frac{O(n^2)}{\mathcal{W}(\sigma') \mathcal{Z}(\Omega)} \sum_{\eta \in H_{\sigma'}} \mathcal{W}(\sigma') \mathcal{W}(\sigma' \oplus \eta) \\ & = \max_{\sigma' \in \Omega} \frac{O(n^2)}{\mathcal{Z}(\Omega)} \sum_{\eta \in H_{\sigma'}} \mathcal{W}(\sigma' \oplus \eta) \\ & \leq \frac{O(n^2)}{\mathcal{Z}(\Omega)} \sum_{\sigma \in \Omega'} \mathcal{W}(\sigma) \\ & = O(n^2) \frac{\mathcal{Z}(\Omega')}{\mathcal{Z}(\Omega)}. \end{aligned}$$

By a standard argument as in [16, 27, 26],  $\frac{\mathcal{Z}(\Omega_4)}{\mathcal{Z}(\Omega_2)} \leq \frac{\mathcal{Z}(\Omega_2)}{\mathcal{Z}(\Omega_0)}$ . Therefore, the congestion is bounded by  $O(n^2) \frac{\mathcal{Z}(\Omega_2)}{\mathcal{Z}(\Omega_0)}$ .

REMARK 4.1. We have an alternative derivation of Lemma 4.1 using the notion of “windability” [26]. However, this alternative derivation does not yield a proof of Theorem 4.1; we still require the results from Section 3 to show that. Readers are referred to [5] for details.

In order to show  $\mathcal{MC}$  is rapidly mixing, we need to show  $\frac{\mathcal{Z}(\Omega_2)}{\mathcal{Z}(\Omega_0)}$  is polynomially bounded. This bound is also needed to get an FPRAS from a rapidly mixing Markov chain in  $\Omega$ , since ultimately we are only interested in  $\Omega_0$ . Such a bound is a corollary of Theorem 3.1.

COROLLARY 4.1.  $\frac{\mathcal{Z}(\Omega_2)}{\mathcal{Z}(\Omega_0)} = O(n^2)$ .



(a) A state in  $\Omega_2$  with  $(=)_2$  's at  $v'$  and  $v''$ . (b) A 4-ary construction made by deleting  $v'$  and  $v''$ .

Figure 7

Proof. For each  $\sigma \in \Omega_2$ , there are exactly two vertices in  $V$  satisfying  $(=)_2$ . Let  $\Omega_2^{\{v', v''\}} \subseteq \Omega_2$  be the set of states in which  $v', v''$  are these two vertices. We have  $\frac{\mathcal{Z}(\Omega_2)}{\mathcal{Z}(\Omega_0)} = \sum_{\{v', v''\} \in \binom{V}{2}} \frac{\mathcal{Z}(\Omega_2^{\{v', v''\}})}{\mathcal{Z}(\Omega_0)}$ . For any  $\sigma \in \Omega_2^{\{v', v''\}}$ , the

local assignments around  $v'$  and  $v''$  must be 00 on one and 11 on the other. An example is in Figure 7a. If we “delete”  $v'$  and  $v''$  as shown in Figure 7b, we get a 4-ary construction  $g$  using degree 4 vertices with constraint functions in  $\mathcal{F}_{\leq 2} \subset \mathcal{F}_{\leq}$ . Denote the constraint matrix of  $g$  by  $M(g) = \begin{bmatrix} & b' & c' & a' \\ a' & c' & b' & \end{bmatrix}$ , with the input order being counter-clockwise starting from the upper-left edge. For this 4-ary construction  $g$  we observe that: the states in  $\Omega_2^{\{v', v''\}}$  where edges incident to  $v'$  (also  $v''$ ) take the same value contribute a total weight  $(a' + a')$ , i.e.  $\mathcal{Z}(\Omega_2^{\{v', v''\}}) = 2a'$ ; the states in  $\Omega_0$  where  $v', v''$  satisfy  $(\neq_2)$  have a total weight  $\mathcal{Z}(\Omega_0) = 2b' + 2c'$ . Note that  $\mathcal{F}_{\leq 2} \subset \mathcal{F}_{\leq}$ . By Theorem 3.1 we know that for 4-ary construction  $g$ ,  $a' \leq b' + c'$ . Therefore,  $\frac{\mathcal{Z}(\Omega_2^{\{v', v''\}})}{\mathcal{Z}(\Omega_0)} \leq 1$ . In total,  $\frac{\mathcal{Z}(\Omega_2)}{\mathcal{Z}(\Omega_0)} \leq \binom{|V|}{2}$ .

Combining Lemma 4.1 and Corollary 4.1, we conclude that  $\mathcal{MC}$  is rapidly mixing, and  $\Omega_0$ , the set of valid six-vertex configurations, in total takes a non-negligible proportion in the stationary distribution. As a consequence, we are able to efficiently sample six-vertex configurations according to the Gibbs measure on  $\Omega_0$ , and in the following algorithm we only work with states in  $\Omega_0$ . We design the following algorithm to approximately compute  $Z(\mathcal{F}_{\leq 2})$  via sampling with the directed-loop algorithm  $\mathcal{MC}$ . As we have argued in Section 3, the partition function of the six-vertex models can be viewed as the weighted sum of Eulerian partitions. For a vertex  $v \in U$ , the ratios among different pairings ( $\curvearrowright$ ,  $\curvearrowleft$ , and  $\dashv$ ) in weighted Eulerian partitions can be uniquely determined by the ratios among different orientations (represented by  $a$ ,  $b$ , and  $c$ ) at  $v$ . As long as the partition function is not zero (this can be easily tested in P), there must be a pairing  $\varrho$  showing up at  $v$  with probability at least  $\frac{1}{3}$  among all three pairings. Therefore, running  $\mathcal{MC}$  on  $G$ , we can approximate, with a sufficient  $1/\text{poly}(n)$  precision, the probability of having  $\varrho$  at  $v$ , denoted by  $\text{Pr}_v(\varrho)$ . Denote by  $G_{v, \varrho}$  the graph with  $v$  being split into  $v_1$  and  $v_2$ , each assigned a  $(\neq_2)$  and the edges reconnected according to  $\varrho$ . Write the partition function of  $G_{v, \varrho}$  as  $Z(G_{v, \varrho})$ , we have  $\text{Pr}_v(\varrho) = w(\varrho)Z(G_{v, \varrho})/Z(G)$  which means  $Z(G) = w(\varrho)Z(G_{v, \varrho})/\text{Pr}_v(\varrho)$ . To approximate  $Z(G)$  it suffices to approximate  $Z(G_{v, \varrho})$ , which can be done by running  $\mathcal{MC}$  on  $G_{v, \varrho}$  and recursing. Repeating this process for  $|U|$  steps we decompose the graph  $G$  into the base case, a set of disjoint cycles with even number of vertices, each assigned a  $(\neq_2)$ . The partition function of this cycle graph is just  $2^C$  where  $C$  is the number of cycles. By this self-reduction, the partition function for  $G$  can be approximated.

Therefore, Theorem 4.1 is proved. Note that for the special case  $(1, 1, 1)$ , the FPRAS by Mihail and Winkler is a reduction [27] to computing the number of perfect matchings in a bipartite graph. We give a direct algorithm using Markov chain Monte Carlo.

**REMARK 4.2.** *After this paper was posted, it has been suggested that one can find an alternative algorithm for the interior of the blue region by adapting and combining the algorithm in [18] and the reduction in [27], although this approach would produce a slightly worse running time. Together with our direct approximation algorithm, this further delineates the blue region as being possibly an intrinsic barrier.*

### 5 Hardness

**THEOREM 5.1.** *If  $f \in \mathcal{F}_{>}$ , then  $Z(f)$  does not have an FPRAS unless  $\text{RP} = \text{NP}$ .*

*Proof.* Let 3-MIS denote the NP-hard problem of computing the cardinality of a maximum independent set in a 3-regular graph [9]. We reduce 3-MIS to approximating  $Z(f)$ . Since  $f \in \mathcal{F}_{>}$ , all  $a, b, c > 0$ . Since the proof of NP-hardness for  $Z(f)$  is for general graphs (i.e., not necessarily planar), we can permute the parameters so that  $c > a + b$ , and normalize  $c > b \geq a = 1$ . Let  $\gamma = \frac{c}{a+b}$ . Then  $\gamma > 1$ .

Before proving this theorem we briefly state our idea. Denote an instance of 3-MIS by  $G = (V, E)$ . For any independent set, no two adjacent vertices  $u, v \in V$  can both appear. The only possible configurations for adjacent  $\{u, v\}$  in any independent set  $S$  are  $(u \in S, v \notin S)$ ,  $(u \notin S, v \in S)$ , and  $(u \notin S, v \notin S)$ . We want to encode this local constraint by a local fragment of a graph  $G'$  in terms of configurations in the six-vertex model.

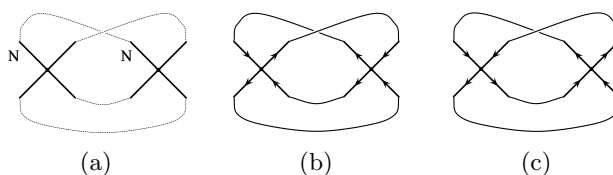


Figure 8: A construction implementing a single edge in an independent set.

In Figure 8a we show how to implement a toy example—a single edge  $\{u, v\}$ —by a construction in the six-vertex model with parameters  $(a = 1, b \geq 1, c > a + b)$ . We create two vertices, the left one for  $u$  and the right one for  $v$ , both given the constraint function  $f$ , and connect them as is shown in Figure 8a. The order of the 4 edges at each vertex is aligned to Figure 1 by a rotation so that the northwest edge marked by

“N” corresponds to the north edge in Figure 1. There are a total of 4 edges in Figure 8a. Every 2-in 2-out configuration on the left vertex uniquely extends to a 2-in 2-out configuration on the right, and vice versa. Hence there are a total of 6 valid configurations. When the left vertex has a saddle configuration (in-out-in-out, or its reversal) which has weight  $c$ , the right must have a non-saddle configuration of weight  $b$ . Figure 8b depicts one such configuration; reversing all arrows gives another one having the same weight. Similarly if the right vertex has a saddle configuration (or its reversal) having weight  $c$  then the left must be a non-saddle having weight  $b$ . There are two more configurations with two non-saddles (Figure 8c and its reversal); these both have weight  $a^2 = 1$ . This models how two adjacent vertices interact in 3-MIS. We will call the connection pattern described in Figure 8a between two sets of 4 dangling edges the *four-way connection*.

However, when a vertex in  $G$  has more than one neighbor, simply duplicating this elementary implementation will not work, because we cannot make sure that the duplicate copies corresponding to the same vertex  $v$  behave consistently. To handle this difficulty, we design a locking device (Figure 9) for every  $v \in V$  such that the property whether  $v$  belongs to an independent set in  $G$  is consistently reflected in  $G'$  in terms of being in a saddle configuration or not. This locking mechanism is enforced in the sense of approximation.

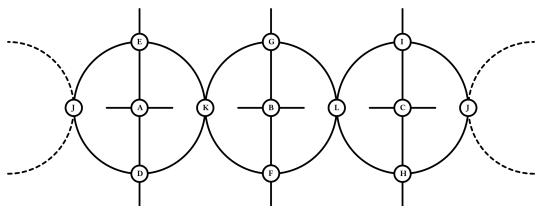


Figure 9: A locking device implementing a degree three vertex and its incident edges.

In Figure 9, we identify the leftmost node  $J$  with the rightmost node  $J$ —there are three “circles” in total. Most nodes depicted in Figure 9 will be replaced by some construction implementing the locking mechanism. Each circle has 4 dangling edges. The “left circle” has two dangling edges incident to  $A$ , one incident to  $D$ , and one incident to  $E$ . Similarly for the “middle circle” and the “right circle”. Each edge  $\{u, v\}$  in  $G$  is modeled by a four-way connection of the 4 dangling edges between one circle of the construction for  $u$  and another circle of the construction for  $v$ . The 4 dangling edges of any circle is said to be in a saddle (or non-saddle) configuration if it is so when viewed externally in the cyclic order depicted in Figure 9.

The locking mechanism is to realize the following: when the four dangling edges of one of the 3 circles take a saddle configuration, (either in-out-in-out, or out-in-out-in), the other two circles must also take the *identical* saddle configuration (in-out-in-out, or out-in-out-in, respectively); when one circle takes any non-saddle configuration, the other two circles can take independently any non-saddle configurations, with no linkage (aside being a non-saddle). This is made possible by *chaining*, and the guarantee is enforced by approximate counting.

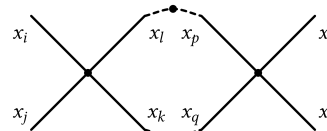


Figure 10: 2-chain.

Figure 10 depicts a *2-chain*. We place the constraint function ( $\neq 2$ ) on the two degree 2 vertices connecting the two degree 4 vertices, each assigned a copy of  $f$ , and the edges are ordered so that  $M = M_{x_i x_j, x_l x_k}(f) = M_{x_p x_q, x_s x_r}(f) = \begin{bmatrix} a & b & c \\ b & a & c \\ c & & \end{bmatrix}$ . Then the constraint function  $f_2$  of this 2-chain construction is obtained by matrix multiplication  $M(f_2) = M_{x_i x_j, x_s x_r}(f_2) = M N M$ , where  $N = \begin{bmatrix} 1 & 1 \\ 1 & 1 \end{bmatrix}$ . Thus  $M(f_2) = \begin{bmatrix} a_2 & b_2 & c_2 \\ b_2 & a_2 & c_2 \end{bmatrix} = \begin{bmatrix} 2ab & a^2+b^2 & c^2 \\ a^2+b^2 & 2ab & c^2 \end{bmatrix}$ , where  $c_2 = c^2$ ,  $a_2 + b_2 = (a + b)^2$ .

Thus  $c_2 > a_2 + b_2$ , and  $\gamma_2 := \frac{c_2}{a_2+b_2} = \left(\frac{c}{a+b}\right)^2 = \gamma^2$ .

This can be generalized to a  $k$ -chain, which connects  $k$  vertices with constraint function  $f$  by  $k - 1$  copies of  $N$ , such that  $c_k = c^k, a_k + b_k = (a + b)^k, \gamma_k = \gamma^k$ . Notice that when  $c > a + b$ , the ratio  $\frac{c}{a+b}$  can be amplified exponentially in  $k$  in a  $k$ -chain. Therefore, by a chain of polynomially bounded size we can ensure the undesirable configurations are negligible — the 4-ary construction is locked into the only two complementary configurations which  $c$  represents. It can be verified that  $b_k = (\mu^k + \nu^k)/2 \geq a_k = (\mu^k - \nu^k)/2 \geq 1$ , where  $\mu = a + b$  and  $\nu = b - a$ . We can “normalize” a  $k$ -chain by dividing  $a_k$ , so that its parameters are  $\tilde{c}_k = c^k/a_k > \tilde{b}_k = b_k/a_k \geq \tilde{a}_k = 1$ , and the ratio  $\frac{\tilde{c}_k}{\tilde{a}_k + \tilde{b}_k} = \gamma^k$ .

To reduce the problem 3-MIS to approximating  $Z(f)$ , let  $\kappa > \lambda \geq 1$  be two constants that will be fixed later. For each 3-MIS instance  $G = (V, E)$  with  $|V| = n$ , we construct a graph  $G'$  where a device in Figure 9 is created for each  $v \in V$ , and a four-way connection is made for every  $\{u, v\} \in E(G)$ , on the

dangling edges between two circles corresponding to  $\{u, v\}$  as in Figure 8a. For each device in Figure 9, each of the nodes  $A, B, C$  is replaced by a *normalized*  $\lambda n$ -chain to boost the ratio of the saddle configuration over other configurations; each of the nodes  $D, F, H$  is replaced by a  $\kappa n^2$ -chain to lock in the configuration “all arrows pointing up and right” and its reversal; each of the nodes  $E, G, I$  is also replaced by a  $\kappa n^2$ -chain to lock in the configuration “all arrows pointing down and right” and its reversal (these configurations at  $D, F, H$ , and at  $E, G, I$  respectively, will be called locking configurations); at each of  $J, K, L$ , we just put  $f$ , of which the maximum weight of a configuration over the minimum is a constant  $\frac{c}{\min\{a,b\}} = c$ . Note that the constraint function in Figure 10 has the dominating entry at 0011 and 1100. Since our graph  $G'$  does not need to be planar, we can reorder the 4 external edges arbitrarily. In particular, for  $A, B, C$  the dominating entry  $\tilde{c}_{\lambda n}$  is in the saddle 0101 and 1010 positions, as depicted in Figure 9. Similarly the 4 external edges of  $D, F, H$  and  $E, G, I$  are also properly reordered from the order given in Figure 10, as a  $\kappa n^2$ -chain to achieve the proper locking configurations.

Next we argue that the maximum size  $s$  of independent sets in  $G$  can be recovered from an approximate solution to  $Z(G'; f)$ .

Given an independent set  $S \subset V$  of size  $s$ , we show there is a valid configuration (at the granularity of nodes and edges shown in Figure 9) of weight  $\geq c^{\delta \kappa n^3} (\tilde{c}_{\lambda n} \tilde{b}_{\lambda n})^{3s}$ . For any vertex  $v \in S$  we set the following configuration for its locking device: set each of 3 nodes  $A, B, C$  to the same saddle configuration in-out-in-out cyclically starting from the upper edge—each has weight  $\tilde{c}_{\lambda n}$ ; set each of 3 nodes  $D, F, H$  to the same out-out-in-in locking configuration (clockwise) cyclically starting from the upper edge—each has weight  $c^{\kappa n^2}$ ; set each of 3 nodes  $E, G, I$  to the same in-out-out-in locking configuration (clockwise) cyclically starting from the upper edge—each also has weight  $c^{\kappa n^2}$ ; set each of 3 nodes  $J, K, L$  to the same configuration “two in from the left and two out to the right”, which has a non-zero weight  $\geq 1$ . For any vertex  $v \notin S$  we set the following configuration for its locking device: All  $D, F, H, E, G, I$  will be in some locking configurations. Consider any of the 3 circles in the device, for example the circle formed by  $A, D, E, J, K$ . The node  $A$  is involved in a four-way connection to another circle belonging to a device for some vertex  $u$ . If  $u \in S$ , the assigned configuration just defined at  $u$  forces a non-saddle configuration here; more specifically the horizontal two dangling edges at  $A$  must either both point right (or both point left), and the upper edge  $\hat{e}$  of  $E$  and the lower edge  $\underline{e}$  of  $D$  must

either both point down (or both point up, respectively). Regardless of which of the two assignments for the pair  $(\hat{e}, \underline{e})$ , either both down or both up, we can assign a locking configuration for  $E$  and  $D$  so that the upper and lower edges of  $A$  are either both point down or both point up respectively, inheriting the orientation at  $(\hat{e}, \underline{e})$ . Note that in either case, the left two edges of  $K$  are one-in-one-out; similarly the right two edges of  $J$  are also one-in-one-out (this allows “freedom” between the 3 circles where each of  $J, K, L$  can take a nonzero weight  $\geq 1$ ). Continuing our description at the circle  $A, D, E, J, K$ , if  $u \notin S$ , then we will pick an arbitrary non-saddle to non-saddle configuration in the four-way connection for  $\{u, v\}$ . These can all be extended to a valid configuration at  $A, D, E$  such that the configuration at  $A$  is non-saddle having weight  $\geq 1$ , the configurations at  $D$  and  $E$  are locking, and the right two edges of  $J$  and the left two edges of  $K$  are both one-in-one-out. The weight at  $D$  and  $E$  are still  $c^{\kappa n^2}$ . Because  $J$  and  $K$  each has one-in-one-out from within the side of the circle, the 3 circles can be assigned independently from each other. This allows us to handle the situation where, for the same  $v \notin S$ , some edge  $\{v, u\}$  connects to  $u \in S$  and some edge  $\{v, u'\}$  connects to  $u' \notin S$ .

We have defined a valid configuration, and it has weight  $\geq \prod_{v \in V} c^{6\kappa n^2} \prod_{v \in S} (\tilde{c}_{\lambda n} \tilde{b}_{\lambda n})^3 = c^{6\kappa n^3} (\tilde{c}_{\lambda n} \tilde{b}_{\lambda n})^{3s}$ , where 6 comes from the 6 locking nodes  $D, E, F, G, H, I$  in each locking device. (Omitted factors are all  $\geq 1$ .)

Next we show that the weighted sum of all configurations is smaller than  $\frac{1}{2} c^{6\kappa n^3} (\tilde{c}_{\lambda n} \tilde{b}_{\lambda n})^{3(s+1)}$ , where  $s$  is the maximum size of independent sets in  $G$ . First we bound  $W_{\text{lock}}$ , the sum of weights for configurations where all nodes labeled  $D, E, F, G, H, I$  are locked. Consider any circle such as the one labeled  $A, D, E, J, K$  for any  $v \in V$ . It is involved in a four-way connection with another such circle for a vertex  $u \in V$ , say  $A', D', E', J', K'$ , where  $\{u, v\} \in E(G)$ . The fact that  $D$  is locked forces that the upper and lower edges of  $D$  are to be consistently oriented, i.e., both up or both down. Similarly, consistency holds at  $E, D'$  and  $E'$ . Thus the four-way connection forces that there can be at most one of  $A$  and  $A'$  is in a saddle configuration. Furthermore, if  $A$  is in a particular saddle configuration, say in-out-in-out starting from the upper edge, both upper and lower edges of  $D$  must point up, and both upper and lower edges of  $E$  must point down, and then both right edges of  $D$  and  $E$  must point right, causing the left two edges of  $K$  point in, and thus the right two edges of  $K$  point out. This forces both  $F$  and  $G$  to take *exactly* the same

locked configurations of  $D$  and  $E$  respectively, which forces  $B$  to be in *exactly* the same saddle configuration as  $A$ . Similarly so is  $C$ . We conclude that when all nodes labeled  $D, E, F, G, H, I$  are locked, for any  $v \in V$ , if any of its  $A, B, C$  is in a saddle configuration, then all 3 are in exactly the same saddle configuration, and none of  $A', B', C'$  for  $u \in V$  is a saddle, if  $\{u, v\} \in E$ . In particular, there can be at most  $3s$  many saddles among  $A, B, C$ 's in  $G'$ . If  $0 \leq i \leq s$  is the number of  $\{A, B, C\}$ 's being in saddle, their weight is  $(\tilde{c}_{\lambda n})^{3i}$ , and their corresponding non-saddles in respective four-way connections must take weight  $(\tilde{b}_{\lambda n})^{3i}$ . Those  $(3n - 6i)/2$  pairwise four-way connections (here  $(3n - 6i)/2$  is an integer, as  $n = |V|$  is even for a 3-regular graph  $G$ ) between two non-saddles have weight  $\tilde{a}_{\lambda n} = 1$ . Note that, if any of those non-saddles were to take weight  $\tilde{b}_{\lambda n}$ , then the corresponding paired node in its four-way connection must be in saddle, a contradiction.

It follows that

$$\begin{aligned} W_{\text{lock}} &\leq 2^{6n} (c^{\kappa n^2})^{6n} \sum_{i=0}^s \binom{n}{i} (\tilde{c}_{\lambda n} \tilde{b}_{\lambda n})^{3i} c^{3n} \\ &\leq 2^{7n} c^{6\kappa n^3 + 3n} (\tilde{c}_{\lambda n} \tilde{b}_{\lambda n})^{3s}, \end{aligned}$$

where each locked node  $D, E, F, G, H, I$  has  $2$  possible locking configurations each with weight  $c^{\kappa n^2}$ , and given a particular assignment of  $6n$  locking configurations, there can be at most  $s$  batches of  $A, B, C$ 's in saddle configurations (same for each batch and determined by the locks) with weight  $\tilde{c}_{\lambda n}$ . Hence  $W_{\text{lock}} < \frac{1}{4} c^{6\kappa n^3} (\tilde{c}_{\lambda n} \tilde{b}_{\lambda n})^{3(s+1)}$ , when  $\lambda \geq 1$  is large.

It remains to upper-bound the weighted sum of configurations where there is at least one device with some lock broken. This quantity is bounded by

$$\begin{aligned} &\sum_{i=0}^{6n-1} \binom{6n}{i} c^{i\kappa n^2} (a+b)^{(6n-i)\kappa n^2} 6^{6n} \\ &\quad \times \left[ 2(\tilde{c}_{\lambda n} + \tilde{b}_{\lambda n} + 1) \right]^{3n} [2(a+b+c)]^{3n} \\ &\leq 2^{30n} (a+b)^{6\kappa n^3} \left( \frac{c}{a+b} \right)^{(6n-1)\kappa n^2} \\ &\quad \times \left[ \tilde{c}_{\lambda n} + \tilde{b}_{\lambda n} + 1 \right]^{3n} [a+b+c]^{3n} \\ &\leq 2^{30n} [\Theta(1)]^{\lambda n^2} c^{6\kappa n^3} \frac{1}{c^{\kappa n^2}} (a+b)^{\kappa n^2} \\ &= 2^{30n} [\Theta(1)]^{\lambda n^2} c^{6\kappa n^3} \frac{1}{\gamma^{\kappa n^2}}, \end{aligned}$$

which is  $< \frac{1}{4} c^{6\kappa n^3}$  when  $\kappa \gg \lambda \geq 1$  is large. Here  $\Theta(1)$  is a constant depending only on  $a, b, c$ , and  $6^{6n}$  comes from

six possible valid configurations for at most  $6n$  vertices of the type  $D, E, F, G, H, I$ , not necessarily in locking configurations.

## 6 Open problems

The main open problem on the approximate complexity of the six-vertex model is in the white region. The finer classification of the approximate complexity for the planar case is also open. Approximating  $T(G; 3, 3)$  is #BIS-hard for general graphs [10]. On planar graphs,  $T(G; 3, 3)$  is equivalent to the six-vertex model at  $(1, 1, 2)$  where the approximation complexity for planar graphs is unknown.

## References

- [1] G. T. Barkema and M. E. J. Newman. Monte carlo simulation of ice models. *Phys. Rev. E*, pages 1155–1166, 1998.
- [2] R. J. Baxter. *Exactly Solved Models in Statistical Mechanics*. Academic Press Inc., San Diego, CA, USA, 1982.
- [3] Jin-Yi Cai, Zhiguo Fu, and Shuai Shao. A complexity trichotomy for the six-vertex model. *CoRR*, abs/1704.01657, 2017.
- [4] Jin-Yi Cai, Zhiguo Fu, and Mingji Xia. Complexity classification of the six-vertex model. *Information and Computation*, 259:130 – 141, 2018.
- [5] Jin-Yi Cai, Tianyu Liu, and Pinyan Lu. Approximability of the six-vertex model. *CoRR*, abs/1712.05880, 2017.
- [6] Martin Dyer, Alan Frieze, and Ravi Kannan. A random polynomial-time algorithm for approximating the volume of convex bodies. *J. ACM*, 38(1):1–17, January 1991.
- [7] Joanna A. Ellis-Monaghan and Criel Merino. Graph polynomials and their applications I: The Tutte polynomial. In Matthias Dehmer, editor, *Structural Analysis of Complex Networks*, pages 219–255. Birkhäuser Boston, Boston, 2011.
- [8] Chungpeng Fan and F. Y. Wu. General lattice model of phase transitions. *Phys. Rev. B*, 2:723–733, Aug 1970.
- [9] M.R. Garey, D.S. Johnson, and L. Stockmeyer. Some simplified NP-complete graph problems. *Theoretical Computer Science*, 1(3):237 – 267, 1976.
- [10] Leslie Ann Goldberg and Mark Jerrum. Approximating the partition function of the ferromagnetic Potts model. *J. ACM*, 59(5):25:1–25:31, November 2012.
- [11] Leslie Ann Goldberg, Russell Martin, and Mike Paterson. Random sampling of 3-colorings in  $\mathbb{Z}^2$ . *Random Structures & Algorithms*, 24(3):279–302, 2004.
- [12] Heng Guo and Tyson Williams. The complexity of planar Boolean #CSP with complex weights. In *Proceedings of the 40th International Colloquium on Automata, Languages, and Programming, ICALP '13*,

- pages 516–527, Berlin, Heidelberg, 2013. Springer Berlin Heidelberg.
- [13] Sangxia Huang and Pinyan Lu. A dichotomy for real weighted Holant problems. *Computational Complexity*, 25(1):255–304, March 2016.
- [14] F. Jaeger. On transition polynomials of 4-regular graphs. In Geña Hahn, Gert Sabidussi, and Robert E. Woodrow, editors, *Cycles and Rays*, pages 123–150. Springer Netherlands, Dordrecht, 1990.
- [15] Mark Jerrum. *Counting, Sampling and Integrating: Algorithm and Complexity*. Birkhäuser, Basel, 2003.
- [16] Mark Jerrum and Alistair Sinclair. Approximating the permanent. *SIAM Journal on Computing*, 18(6):1149–1178, 1989.
- [17] Mark Jerrum and Alistair Sinclair. Polynomial-time approximation algorithms for the ising model. *SIAM Journal on Computing*, 22(5):1087–1116, 1993.
- [18] Mark Jerrum, Alistair Sinclair, and Eric Vigoda. A polynomial-time approximation algorithm for the permanent of a matrix with nonnegative entries. *J. ACM*, 51(4):671–697, July 2004.
- [19] Mark R. Jerrum, Leslie G. Valiant, and Vijay V. Vazirani. Random generation of combinatorial structures from a uniform distribution. *Theoretical Computer Science*, 43(Supplement C):169 – 188, 1986.
- [20] Richard M. Karp and Michael Luby. Monte-Carlo algorithms for enumeration and reliability problems. In *Proceedings of the 24th Annual Symposium on Foundations of Computer Science*, SFCS '83, pages 56–64, Washington, DC, USA, 1983. IEEE Computer Society.
- [21] Greg Kuperberg. Another proof of the alternating-sign matrix conjecture. *International Mathematics Research Notices*, 1996(3):139–150, 1996.
- [22] Elliott H. Lieb. Exact solution of the  $F$  model of an antiferroelectric. *Phys. Rev. Lett.*, 18:1046–1048, Jun 1967.
- [23] Elliott H. Lieb. Exact solution of the two-dimensional slater KDP model of a ferroelectric. *Phys. Rev. Lett.*, 19:108–110, Jul 1967.
- [24] Elliott H. Lieb. Residual entropy of square ice. *Phys. Rev.*, 162:162–172, Oct 1967.
- [25] Michael Luby, Dana Randall, and Alistair Sinclair. Markov chain algorithms for planar lattice structures. *SIAM Journal on Computing*, 31(1):167–192, 2001.
- [26] Colin McQuillan. Approximating Holant problems by winding. *CoRR*, abs/1301.2880, 2013.
- [27] M. Mihail and P. Winkler. On the number of Eulerian orientations of a graph. *Algorithmica*, 16(4):402–414, Oct 1996.
- [28] Linus Pauling. The structure and entropy of ice and of other crystals with some randomness of atomic arrangement. *Journal of the American Chemical Society*, 57(12):2680–2684, 1935.
- [29] Nikolay Prokof'ev and Boris Svistunov. Worm algorithms for classical statistical models. *Phys. Rev. Lett.*, 87:160601, Sep 2001.
- [30] Aneesur Rahman and Frank H. Stillinger. Proton distribution in ice and the kirkwood correlation factor. *The Journal of Chemical Physics*, 57(9):4009–4017, 1972.
- [31] Dana Randall and Prasad Tetali. Analyzing Glauber dynamics by comparison of Markov chains. *Journal of Mathematical Physics*, 41(3):1598–1615, 2000.
- [32] Alistair Sinclair. Improved bounds for mixing rates of Markov chains and multicommodity flow. *Combinatorics, Probability and Computing*, 1:351–370, 1992.
- [33] J. C. Slater. Theory of the transition in  $\text{KH}_2\text{PO}_4$ . *The Journal of Chemical Physics*, 9(1):16–33, 1941.
- [34] Bill Sutherland. Exact solution of a two-dimensional model for hydrogen-bonded crystals. *Phys. Rev. Lett.*, 19:103–104, Jul 1967.
- [35] Olav F. Syljuåsen and M. B. Zvonarev. Directed-loop monte carlo simulations of vertex models. *Phys. Rev. E*, 70:016118, Jul 2004.
- [36] W. T. Tutte. A contribution to the theory of chromatic polynomials. *Canad. J. Math.*, 6(0):80–91, January 1954.
- [37] Michel Las Vergnas. On the evaluation at  $(3, 3)$  of the Tutte polynomial of a graph. *Journal of Combinatorial Theory, Series B*, 45(3):367 – 372, 1988.
- [38] A. Yanagawa and J.F. Nagle. Calculations of correlation functions for two-dimensional square ice. *Chemical Physics*, 43(3):329 – 339, 1979.
- [39] Doron Zeilberger. Proof of the alternating sign matrix conjecture. *Electronic Journal of Combinatorics*, 3(2), 1996.